Vol. 06, No. 4 (2024) 1857-1864, doi: 10.24874/PES.SI.25.03b.007

Proceedings on Engineering Sciences

www.pesjournal.net

VARIABILITY OF IONOSPHERIC F2 REGION DUE TO SUDDEN STRATOSPHERIC WARMING EVENT OF 2017

Qadeer Ahmed
Anshul Singh
N. Praneetha
Ankit Gupta
Arti Bhardwaj
Puja Goel
A. K. Upadhayaya[1]

Received 28.11.2023.
Received in revised form 07.01.2024.
Accepted 10.02.2024.
UDC – 550.388.2

Keywords:

Sudden Stratospheric Warming (SSW), Ionosphere, Electron Density, Stratospheric Temperature, Quasi-Stationary Planetary Waves

A B S T R A C T

We analyzed the impact of minor Arctic sudden stratospheric warming (SSW) event of 2017 on the ionospheric F2 region, using Digisonde data from a low-mid latitude Indian station, Delhi (28.6°N, 77.2°E, 19.2°N geomagnetic latitude, 42.4°N dip). Our study revealed significant ionospheric changes, with electron densities exhibiting variations of more than 200% during this warming event. To further investigate, we examined the deviation in critical frequency ΔfoF2 from median values in the first six months of 2017 and found that the F2 layer critical frequency experiences maximum and minimum variations during the SSW period. Additionally, we observed periodicities of 7, 11, 14 and 30 days in characteristic F2 layer frequency during this event.

1. INTRODUCTION

Ionosphere is the part of Earth's upper atmosphere extending from ~ 60km to above 500km, mainly created by incoming high frequency solar radiations (EUV and X-ray) and the particle precipitation from the Sun. Significant numbers of electrons and ions that are present in the ionosphere influence the radio signals, satellite signals and Global Navigation Satellite Systems (GNSS) passing through it. One of the primary causes of error in GPS precise positioning and navigation is the ionospheric delay in the propagation of GPS signals. However, ionosphere shows variability in density, composition, and distribution of the ionized gases over time that causes delay in GPS signal and results in positioning error in single frequency GPS. Yu & Liu, 2021 reported ~7.1 to~7.9 times positioning error relative to ionospheric quite day in GPS signal during 2013 tropical cyclone Usagi event in the Hong Kong region. Besides the diurnal and seasonal variations, ionosphere undergoes changes during severe space weather events such as solar flares and geomagnetic storms (Uma et al., 2012). In addition to the upper

[1] Corresponding author: A K. Upadhyaya
Email: upadhayayaak@nplindia.org

atmospheric phenomena such as solar flares and geomagnetic storms known for primarily perturbing the ionosphere, ionospheric variability is also driven by planetary waves, gravity waves under stable solar and geomagnetic conditions (Hocke & Schlegel, 1996). Studies such as (Gupta & Upadhayaya, 2017; Tulasi Ram et al., 2017) reported ionospheric variability associated with seismological events.

Among the other lower atmospheric phenomenon Sudden Stratospheric Warming is one such phenomenon known to perturb the ionosphere. Sudden stratospheric warming that was first observed by Scherhag in 1952, is a meteorological phenomenon when polar stratospheric temperature during the winters increases by up to ~50°C within a few days accompanied by alteration of wind circulation pattern. This phenomenon is more prominent in northern hemisphere, brought on by planetary-scale waves that travel upward from the troposphere. SSWs have a significant impact on the chemistry, temperatures, winds, neutral (non-ionized) particles and electron densities in the stratosphere that extend beyond mesosphere (Baldwin et al., 2021).

Through dynamical processes, the stratospheric state influences the light-ion dominated protonosphere. The ionosphere's O+ may be transported by upward disturbance drifts to the protonosphere, where it is primarily converted to H+ by chemical coupling and the ionosphere contracts (Zhang et al., 2023). It is known that the tropical upper atmosphere experiences significant changes related to SSW, including an increase in amplitudes of semi-diurnal tides on the order of 10-15 m/s in comparison to the usual period (Susanth, 2021).

Gupta & Upadhayaya, (2017a) investigated ionospheric response to seven SSW events from 2010 to 2016 for wide latitude from 26.6°N to 45.1°N of Asian region and observed the latitudinal dependence of semidiurnal variations and perturbations in ionospheric F2 region in form of enhancements and depressions in electron density.

Recently, Goncharenko et al., 2021 studied the impact of SSW 2019 of southern hemisphere on mid latitude ionosphere (northern hemisphere) and reported anomalies in Total electron content (TEC). Pedatella, 2022 used a combination of Constellation Observing System for Meteorology, Ionosphere, and Climate-2 (COSMIC-2) observations and the Whole Atmosphere Community Climate Model with thermosphere–ionosphere extension (WACCM-X) simulations to investigate the variability in the ionosphere during the 2020–2021 sudden stratospheric warming (SSW) and observed a reduction in the diurnal and zonal mean ionosphere total electron content (ITEC) and decreased amplitude of the diurnal variation in the ionosphere during the SSW.

Most of the studies are carried out at different latitudes except a few studies at Indian latitude. We attempted to quantify the extent of ionospheric perturbation in F2 region associated with sudden stratospheric warming at Indian station Delhi. We found the perturbations in ionosphere in form of enhancements in electron density around the stratospheric warming peak. Further we also examined 6 months data and noticed maximum deviation in critical frequency values during the SSW months.

An important part of our study is that it investigates the pharmacophores model to learn more about how the functional group interacts with the amino acids of the receptor at the molecular level. The utilization of a singular pharmaceutical agent that may effectively target several molecular targets has the potential to be a promising therapeutic approach for the treatment of many types of cancer (Hu et al. 2022). Further, to conduct a molecular docking analysis on the epidermal growth factor receptor (EGFR) using potential lead molecules to forecast their pharmacokinetic characteristics.

2. DATA AND METHODOLOGY

The variation in Ionospheric F2 region following the sudden stratospheric warming is illustrated by critical frequency (foF2) and virtual height (h`F) values obtained after 5 minutes by using Digisonde installed at low-mid latitude Indian station (CSIR-National Physical Laboratory), Delhi (28.6°N, 77.2°E, 19.2°N geomagnetic latitude, 42.4°N dip). Auto scaled Ionograms recorded after every 5 minutes are then manually scaled by using the SAO explorer software. SAO Explorer is the flagship software tool for working with Global Ionosphere Radio Observatory (GIRO) ionograms (https://ulcar.uml.edu/SAO-X/SAO-X.html).To eliminate the diurnal variability, we have then calculated the deviation in critical frequency values (ΔfoF2) by taking the difference of foF2 values from average foF2 values of 5 quiet days. The data of international quiet days can be downloaded from http://www.ga.gov.au/oracle/ geomag/iqd_form.jsp.

The Polar stratospheric parameters like temperature at 90° N and 10hpa level, temperature at 60-90°N, amplitudes of planetary wave1 and planetary wave 2 and mean zonal wind at 60°N are taken from NASA's Global Space Flight Center, available on website http://acdb-ext.gsfc.nasa.gov/Data_services/met/ann_data.html. To calculate peak warmings in stratospheric temperature we have taken the daily average stratospheric temperature from 1979 to 2020 and stratospheric temperature during the SSW period available on above website. For determining the influence of solar and geomagnetic activity on ionosphere during the SSW period, $F_{10.7}$ flux and $K_p$index have been obtained from https://omniweb.gsfc.nasa.gov/form/dx1.html.

To isolate ionospheric variability linked to SSW, seismic data available on India Meteorological Department's website https://riseq.seismo.gov.in/riseq/earthquake is used to check any influence of earthquake events occurring during the SSW period. Following formula have been used to calculate percentage change in electron density for determining enhancement and depression.

$$\Delta N_e = (f_o F_2)^2{}_{obs} - (f_o F_2)^2{}_{avg}$$

$$\text{Change in electron density} = \frac{\Delta N_e}{N_e} \times 100\%$$

Where , $(f_oF_2)_{obs}$ is the f_oF2 values obtained after every 5 minutes and $(f_oF_2)_{avg}$ is the average of 5 quiet days during the month.

The first largest value in stratospheric temperature at 90°N was attained three days following the onset of the warming period. After a slight decrease in temperature by 19K, it showed a second peak after an interval of 6 days. After the recovery phase of the second peak, it remained near the average temperature for 12 days from 09 February to 21 February and again reached a maximum temperature of 255K, where the temperature was enhanced by 35K. Similar variations in stratospheric temperature at 60°-90°N were seen as shown in Fig.1(b).

This event of 2017 was a minor SSW event, as in this case, zonal mean wind at 60°N became weak, as illustrated in Fig 1(c), and the polar vortex shifted off the pole but did

3. OBSERVATIONS

Figure 1 represents the SSW summary i.e., stratospheric temperature, mean zonal wind, solar and geomagnetic conditions prevailing during the SSW event of 2017. The vertical red dashed line in Fig.1 marks the start and end of the warming period. This stratospheric warming at 10hpa level (~32km) remained for 38 days extending from 26 January to 05 March 2017. The black line in Fig 1(a) shows the daily average stratospheric temperature calculated from 1979 to 2017 and the red dotted line shows the stratospheric temperature for the SSW period. During this event maximum increase in stratospheric temperature by ~47K is observed, wherein temperature enhanced from 217K to 264K (as shown in fig.1(a)). Three instances of Peak warming are seen on 29 January, 05 February, and 26 February with temperature anomaly (ΔT) of 42K, 47K and 35K, respectively, in contrast to the average temperature.

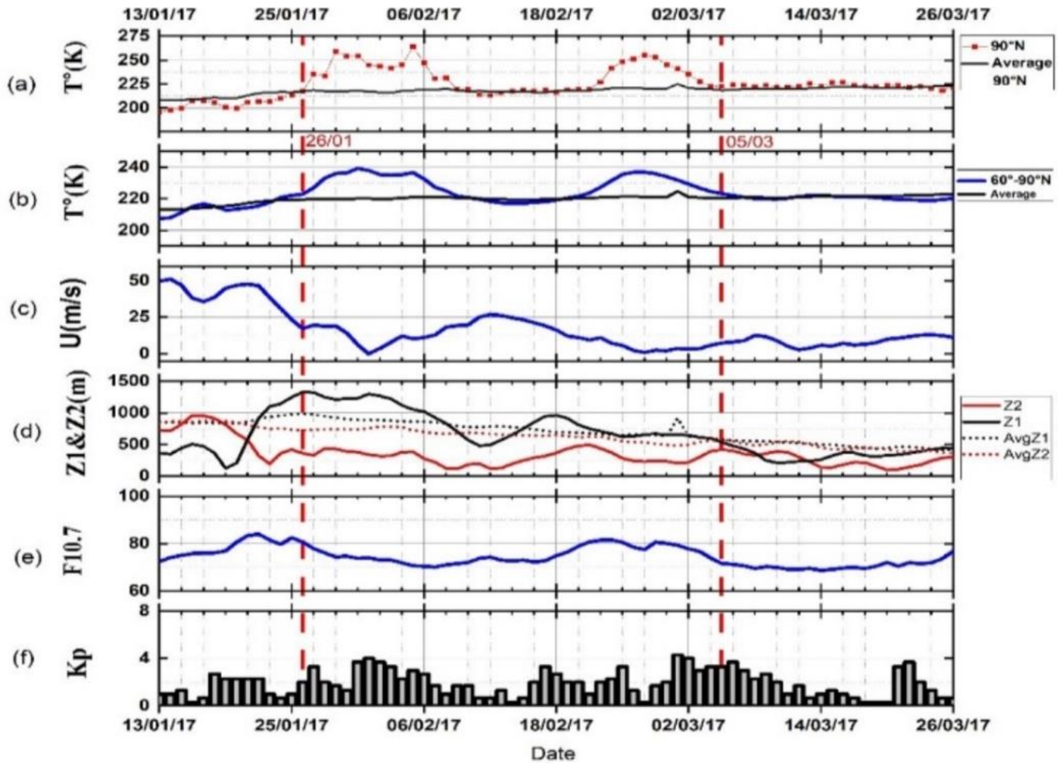

Figure 1. Stratospheric summary during the SSW event of 2017:(a) Stratospheric temperature at 90°N, 10 hPa level (b) zonal mean stratospheric temperature at 60°N–90°N, 10 hPa level (c) Mean zonal wind at 60°N, 10 hPa level, (d) Planetary wave 1 & wave 2 activity at 60°N, 10 hPa level, (e) F10.7 daily average solar radio flux in SFU and (f) daily average Kp index

not change the direction. Figure 1(d) shows amplification in planetary wave Z1 (black line) at 60°N and 10 hPa level beginning from 19 January which continued throughout the warming period. Z1 activity dominates the circulation over Z2 during this SSW period, as illustrated in Fig 1(d). This increased wave activity causes significant changes in the neutral composition of the atmosphere and thus contributes to perturbations in the ionosphere due to the lower atmosphere. The first Maximum peak of planetary wave activity Z1 coincided with the onset of the warming period, and the second peak occurred three days before the beginning of the third peak of stratospheric warming at 90°N.Similarly, the third peak of stratospheric temperature at 90°N coincided with the amplification peak of planetary wave Z. The solar (F10.7 flux) and geomagnetic activity (Kp index) during this period are presented in Figure 1(e) & 1(f), respectively, because the state of the ionosphere is well known to be strongly controlled by solar and geomagnetic activity. To associate ionospheric variability with SSW, other conditions like solar and geomagnetic activity needs to be constant. During this event, the F10.7 flux (~70 to 80 SFU) remained low and stable. Geomagnetic conditions (Kp index) are also considered to investigate the SSW influence on the ionosphere. It can be seen from Figure 1(f) that geomagnetic activity remained quiet (Kp<4, except in one case when Kp =4.3) during this entire period of warming.

To examine ionospheric response during the SSW event of 2017, the critical frequency of the F2 layer (foF2) and deviation in critical frequency (ΔfoF2) from quiet time average from 13 January 2017 to 26 March 2017(2 weeks before and 3 weeks after warming period) is presented in Fig.2, where the vertically drawn red dashed line marks the beginning and ending of SSW event. Peak warming dates (29 January, 05 February and 26Feb) are shown by a solid yellow line in Fig.2. In this case, we assumed variation in ΔfoF2 to be anomalous if $|\Delta foF2| \geq 3.5$MHz, where $\Delta foF2 \leq -3.5$ MHz and $\Delta foF2 \geq 3.5$MHz refers to enhancement and depression respectively, calculated by taking the difference from quiet time average values.

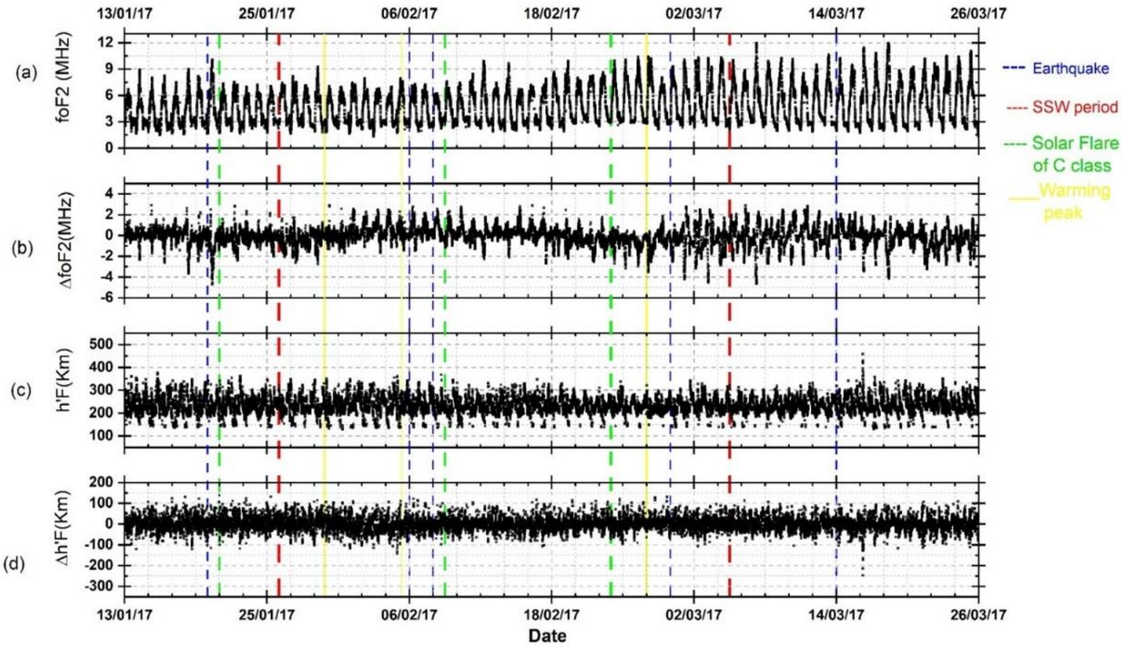

Figure 2. Plot of (a) F2 layer critical frequency (foF2) in MHz (b) Deviation in F2 layer critical frequency (ΔfoF2) from quiet time average (c) Virtual height h`F in Km and (d) Deviation in virtual height from (Δh`F) quiet time average

During this entire duration, we observed 7 cases of enhancement in critical frequency values of the F2 layer, i.e. When $\Delta foF2 \leq -3.5$MHz (shown in table 1). However, no case of depression in foF2 values was found. A maximum enhancement of 4.7MHz from the quiet time average is observed in foF2 (foF2=9.9MHz as shown in table) with the enhancement in electron density by ~260% on 20 January, five days before the start of the warming period, which coincided with an earthquake event shown by blue dotted lines in Fig.2. Another enhancement of 4.5MHz (foF2=10.22MHz) corresponding to enhancement in electron density by 223 % is seen during this warming period on 03 March 2017, which occurred 05 days after the 2nd warming peak.

Two days after the peak warming (26 February), an enhancement of 4.2MHz occurred on 01 March, increasing electron density by ~200%. In addition to these changes, enhancment in foF2 values on other occasions with changes in electron density varying from ~130 % to ~260% (as shown in the table) is seen.

Apart from enhancements in critical frequency values, Virtual height h`F also shows enhancements and depressions during and after the warming period as shown in Figure 2(d). Maximum enhancement of height by 247km compared to the average quite time value was seen on 16 March, 11 days after the warming period. Maximum depression in h`F by 132km is observed on 27 February, a day after third warming peak.

Table 1.Cases of enhancement in critical frequency values during SSW event of 2017.

Date	Time	foF2	Average foF2	ΔfoF2	% Change in electron density
20-01-2017	09:15:00	9.9	5.2	-4.7	259
03-03-2017	04:55:00	10.2	5.6	-4.5	223
01-03-2017	04:45:00	10	5.8	-4.2	199
18-01-2017	09:40:00	8.8	5.1	-3.6	196
07-03-2017	06:35:00	11.9	7.3	-4.6	167
18-03-2017	10:15:00	11.7	7.5	-4.1	140
26-02-2017	03:55:00	10.3	6.8	-3.5	130

4. RESULTS AND DISCUSSION

This work focuses on ionospheric response of F2 region to the minor SSW event of 2017 at low mid latitude Indian station Delhi. In this analysis we have shown variations in F2 layer critical frequency (foF2) and virtual height h`F following this event. Anomalous behavior in terms of enhancement was found in both foF2 and h`F. The SSW event of 2017 showed 05 cases of enhancement in foF2 values with change in electron density varying from ~130% to ~223%. A total of 07 cases are observed during the 73 days, out of which 02 cases of enhancement occurred before the SSW event and 05 cases of enhancements are seen during and after the warming period. Virtual height (h`F) also shows enhancement and depression during and after the warming period. Solar and geomagnetic conditions which are primarily known for perturbing the ionosphere remained quiet and stable (F10.7 index<80 and Kp index<4) before and during the warming period which indicates the possibility of SSW perturbing the otherwise neutral composition of atmosphere. (Gupta &Upadhayaya, 2017b) reported seismo-ionospheric coupling perturbing the ionosphere in form of enhancement (3-4 days prior to an earthquake) and depression in F2 layer critical frequency. On the similar pattern we analysed ionospheric variations associated with earthquake events shown by blue dashed line in Fig.2. Out of five cases enhancement in F2 layer critical frequency on one occasion is seen two days prior to the earthquakes (coinciding with warming peak). We also examined deviation in critical frequency ΔfoF2 from median values during the first six months of 2017 presented in Fig.3, where blue dot shows the maximum value of ΔfoF2 during the SSW period red dot shows hourly median of ΔfoF2 values. We found that maximum deviation in critical frequency from median values, particularly from 06:00 to 10:00hrs (LT) occurred during the SSW period of 2017, which points toward the contribution of SSW causing deviation in critical frequency from median values. To check the influence of quasi stationary planetary waves we have performed Lomb-Scargle (illustrated in figure 4) spectral analysis. We utilized the detrended values of F2 layer critical frequency (ΔfoF2) for two weeks before and three weeks after the Sudden Stratospheric Warming (SSW) period, encompassing a total of thirty-eight days during the SSW. The normalized power spectral densities, generated through the Lomb-Scargle periodogram, depict periods where dominant and secondary components of the wave are observed.

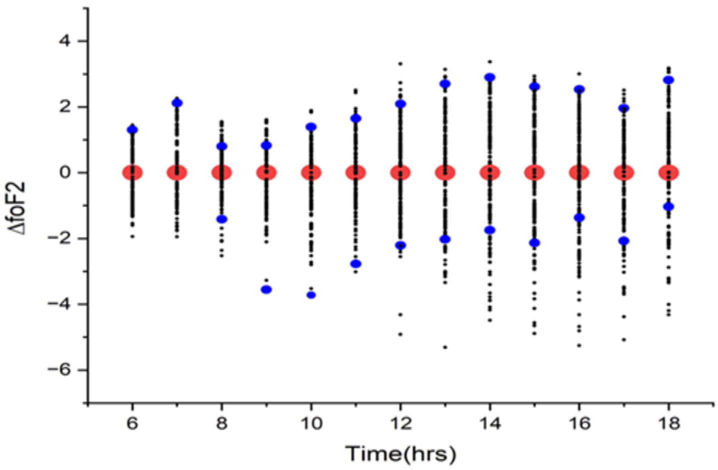

Figure 3. Six months plot of hour wise (0600 to 1800 LT) deviation of critical frequency ΔfoF2 from median values for SSW events of 2017.

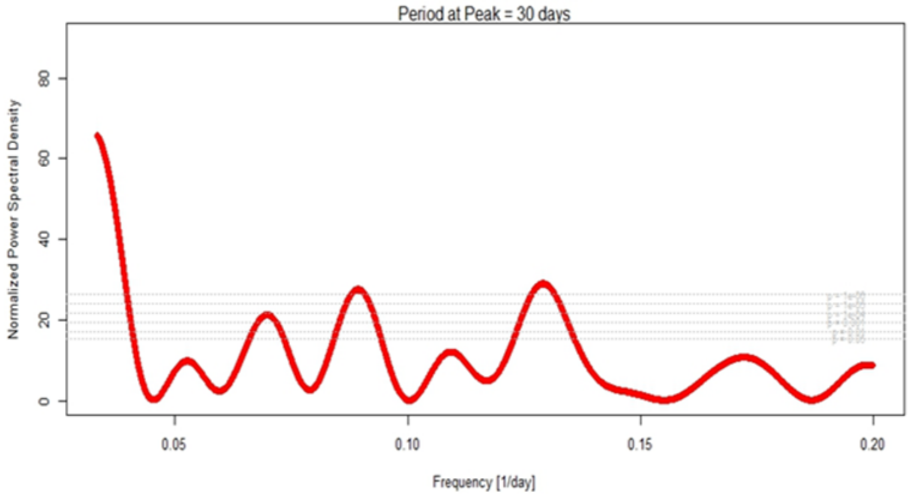

Figure 4. Lomb-Scargle periodogram showing periodicities and period of peak for the SSW events of 2017.

It is essential to highlight that, post-normalization, the spectral power density exhibits an exponential probability distribution with a mean of unity in these plots. We have found peak periodicity of 30 days in addition to the periodicities of 7, 11 and 14 days during the 2017 SSW event. Recently, (Liu et al., 2023)demonstrated that 14 days periodicity is mainly driven by low-level geomagnetic activity represented by Kp index. Several other studies such as (Gupta &Upadhayaya, 2017a; Sripathi &Bhattacharyya, 2012; Upadhayaya & Mahajan, 2013 also reported periodicities ranging from 2 to 30 days. The SSW events are characterized by a rapid increase in temperatures in the stratosphere, particularly over the Polar Regions. This warming can disrupt the usual temperature and pressure patterns in the upper atmosphere, leading to vertical coupling that influences the layers below, including the mesosphere and ionosphere. The reports have shown that the SSW events are often associated with the propagation of planetary waves from the troposphere into the stratosphere. These waves can subsequently modulate the atmospheric circulation and temperatures, impacting the ionosphere.

5. CONCLUSION

Despite solar and geomagnetic conditions being quiet and stable we find perceptible ionospheric variations in electron densities during the minor SSW event of 2017 with enhancement in electron density varying from 130% to 223% and enhancements in electron density were pronounced around and during the warming peak. Six-month plot of deviation in critical frequency values from median values also indicates maximum perturbation during the SSW period. It has been observed that SSW brings significant perturbations in F2 region of ionosphere. Thus, we suggest, inclusion of the SSW phenomena in the models for prediction of ionospheric behaviour. However, in order to assess the extent of variability in the ionosphere associated with SSW, it is crucial to investigate additional events.

Acknowledgement: The authors are thankful to CSIR-NPL for providing the research facilities and NASA Goddard space flight Centre for making the data available on its website. The authors are also thankful to CSIR and UGC for granting Fellowship.

References:

Baldwin, M. P., Ayarzagüena, B., Birner, T., Butchart, N., Butler, A. H., Charlton-Perez, A. J., ... & Pedatella, N. M. (2021). Sudden stratospheric warmings. *Reviews of Geophysics*, *59*(1), e2020RG000708. Blackwell Publishing Ltd. doi:10.1029/2020RG000708

Goncharenko, L. P., Harvey, V. L., Greer, K. R., Zhang, S. R., Coster, A. J., & Paxton, L. J. (2021). Impact of September 2019 Antarctic Sudden Stratospheric Warming on Mid-Latitude Ionosphere and Thermosphere Over North America and Europe. *Geophysical Research Letters*, *48*(15). doi:10.1029/2021GL094517

Gupta, S., & Upadhayaya, A. K. (2017a). Morphology of ionospheric F2 region variability associated with sudden stratospheric warmings. *Journal of Geophysical Research: Space Physics*, *122*(7), 7798–7826. doi:10.1002/2017JA024059

Gupta, S., & Upadhayaya, A. K. (2017b). Preearthquake anomalous ionospheric signatures observed at low-mid latitude Indian station, Delhi, during the year 2015 to early 2016: Preliminary results. *Journal of Geophysical Research: Space Physics*, *122*(8), 8694–8719. doi:10.1002/2017JA024192

Hocke, K., & Schlegel, K. (1996). A review of atmospheric gravity waves and travelling ionospheric disturbances: 1982-1995. *Annales Geophysicae*, *14*(9), 917–940. doi:10.1007/s00585-996-0917-6

Liu, H., Otsuka, Y., Hozumi, K., & Yu, T. (2023). Day-to-day variability of the equatorial ionosphere in Asian sector during August–October 2019. *Frontiers in Astronomy and Space Sciences*, *10*. doi:10.3389/fspas.2023.1198739

Pedatella, N. (2022). Ionospheric Variability during the 2020–2021 SSW: COSMIC-2 Observations and WACCM-X Simulations. *Atmosphere*, *13*(3). doi:10.3390/atmos13030368

Sripathi, S., & Bhattacharyya, A. (2012). Quiet time variability of the GPS TEC and EEJ strength over Indian region associated with major sudden stratospheric warming events during 2005/2006. *Journal of Geophysical Research: Space Physics*, *117*(5). doi:10.1029/2011JA017103

Susanth, S. G. (2021). A brief review on the Atmosphere-Ionosphere coupling during Stratospheric sudden warming over the tropical region. *Indian Journal of Science and Technology*, *14*(11), 956–963. doi:10.17485/IJST/v14i11.251

Tulasi Ram, S., Sunil, P. S., Ravi Kumar, M., Su, S. Y., Tsai, L. C., & Liu, C. H. (2017). Coseismic Traveling Ionospheric Disturbances during the Mw 7.8 Gorkha, Nepal, Earthquake on 25 April 2015 From Ground and Spaceborne Observations. *Journal of Geophysical Research: Space Physics*, *122*(10), 10,669-10,685. doi:10.1002/2017JA023860

Uma, G., Brahmanandam, P. S., Kakinami, Y., Dmitriev, A., Latha Devi, N. S. M. P., Uday Kiran, K., Y. H. Chu (2012). Ionospheric responses to two large geomagnetic storms over Japanese and Indian longitude sectors. *Journal of Atmospheric and Solar-Terrestrial Physics*, *74*, 94–110. doi:10.1016/j.jastp.2011.10.001

Upadhayaya, A. K., & Mahajan, K. K. (2013). Ionospheric F2 region: Variability and sudden stratospheric warmings. *Journal of Geophysical Research: Space Physics*, *118*(10), 6736–6750. doi:10.1002/jgra.50570

Yu, S., & Liu, Z. (2021). The ionospheric condition and GPS positioning performance during the 2013 tropical cyclone Usagi event in the Hong Kong region. *Earth, Planets and Space*, *73*(1). doi:10.1186/s40623-021-01388-2

Zhang, R., Liu, L., Chen, Y., Le, H., & Li, W. (2023). The Stratosphere-Ionosphere-Protonosphere Coupling: Evidence From the Ion Composition Observations During the 2009 Sudden Stratospheric Warming. *Geophysical Research Letters*, *50*(2). doi:10.1029/2022GL101707

Qadeer Ahmed
1-Accademy of Scientific andInnovative ResearchGhaziabad,Uttar Pradesh,India
2-CSIR-National Physical Laboratory, New Delhi, India
qahmed785@gmail.com
ORCID 0000-0001-8133-0252

Anshul Singh
1-Accademy of Scientific andInnovativeResearchGhaziabad,Uttar Pradesh, India
2- CSIR-National Physical Laboratory, New Delhi, India
phy.anshul@gmail.com
ORCID 0009-0008-3484-7740

N. Praneetha
Department of CSE
KLEF University,
Vaddeswaram- 522 302, India
nyshpranee@gmail.com
ORCID 0000-0002-7027-9516

Ankit Gupta
1-Accademy of Scientific and Innovative ResearchGhaziabad,Uttar Pradesh, India
2- CSIR-National Physical Laboratory, New Delhi, India
akki.ankitgupta1995@gmail.com
ORCID 0009-0007-2475-5589

Arti Bhardwaj
1-Accademy of ScientificandInnovative ResearchGhaziabad,Uttar Pradesh, India
2- CSIR-National Physical Laboratory, New Delhi, India
arti.bhardwaj0@gmail.com
ORCID 0009-0007-5215-2224

Puja Goel
Physics Department
G. B. Pant University of Agriculture and Technology,
Pantnagar, Uttrakhand- 263145, India
pujagoel@gmail.com
ORCID 0000-0002-4385-2356

Arun Kumar Upadhayaya
CSIR-National Physical Laboratory, New Delhi, India
upadhayayaak@nplindia.org
ORCID 0000-0002-2314-5259